Indian Journal of Pure & Applied Physics
Vol. 62, December 2024, pp. 1106-1112
DOI: 10.56042/ijpap.v62i12.11324

Solar Cells on the Base of Isotype Heterojunction Black Silicon - Crystalline Silicon

Ferdinand Gasparyan[a,b*] & Vladimir Gasparian[c]

[a]Yerevan State University, 1 Alex Manoogian St, 0025, Yerevan, Armenia

[b]National Polytechnic University of Armenia, 105 Teryan St, 0046, Yerevan, Armenia

[c]California State University, Bakersfield, CA 90032, USA

Received 23 May 2024; accepted 6 November 2024

Simulations of the short-circuit current, open-circuit voltage, absorption coefficient, fill factor and power conversion efficiency of a p-type black silicon/p-type crystalline silicon isotype heterojunction were carried out. Such a heterojunction is part of a complex tandem 2T solar cell NiO – Perovskite – TiO_2 – black Si – crystalline Si. The expression used for the current-voltage characteristic of a heterojunction takes into account the electrical, optical and geometric parameters of both crystalline and black silicon. Analytical expressions were obtained for the absorption coefficients for both crystalline (for the wavelength range 700-1100 nm) and black silicon (for the wavelength range 300-700 nm). The best model data obtained for a short-circuit current density of ~31 mA/cm^2 and an open-circuit voltage of ~634 mV are obtained for the wavelength range 500-800 nm and are in good agreement with the results of previous numerical and experimental data for solar cells of similar composition and size. The calculations show the potential possibility of using black silicon in the design of tandem solar cells. The novelty of this work is the demonstration of the possibility of using thin layers of black silicon to convers solar energy. This material provides good absorption of photons with energy >1.4 eV. In combination with the crystalline silicon, black silicon can broaden the absorption spectrum of irradiation, thereby increasing the power conversion efficiency of the tandem solar cells.

Keywords: Black silicon; heterojunction; Solar cell; Short circuit current

1 Introduction

Black silicon (bSi) is a structured surface of silicon, which seems to be black due to the effective reduction of reflection[1]. The surface of black silicon is structured by cones, pyramids and pores[2-4]. The structured surface of silicon not only reduces the reflection of light but also scatters the latter, which increases the optical path of light and its absorption[5]. Black silicon, as a substrate material, does not directly form a heterojunction (HJ), but can form a heterojunction with other materials through element doping or thin film deposition, quantum dots, etc. Element doping brings an intermediate bandgap, and thin film deposition affects the bandgap structure, both of which are equivalent of a decrease of the effective bandgap[6]. In combination with the excellent optoelectronic properties of bSi, these HJs jointly contribute to the high spectral responsivity, high quantum efficiency, and wide spectral response range of bSi photodetectors. Black silicon, as a silicon-based material, has excellent light absorption properties and advantages in achieving high quantum efficiency and sensitivity. A self-biased nanostructured bSi heterojunction photodiode is demonstrated in[7]. Characteristics of bSi based photovoltaic cells and theoretical modeling of photovoltaic cells are carried out in[8]. Recently, the Brookhaven National Laboratory in the United States and the Aalto University in Finland have developed a bSi based UV optoelectronic device with an external quantum efficiency of 96% at 250–900 nm. Thus, the use of bSi as a substrate for the detection of visible and UV light is a very promising and challenging research topic. It has been demonstrated that when used in photodetectors bSi significantly improves photon detection and extends spectral sensitivity from NIR to the visible wavelengths[9, 10].

The first solar cell (SC) using a silicon heterojunction in the form of an hydrogenated amorphous silicon (a-Si:H)/poly-Si heterojunction bottom cell in a tandem junction SC was reported 41 years ago in 1983[11, 12]. Improvements in the performance of single junction silicon HJ solar cells are reported in Ref. [13]. The following values were

*Corresponding author: (E-mail: fgaspar@myyahoo.com)

obtained: Power conversion efficiency (PCE) - 26.81% and open circuit voltage V_{oc} - 751.4 mV, fill factor) FF - 86.07% and short circuit current density J_{sc} 41.45 mA/cm^2, respectively. It is noted that the cell provides an efficiency of 26.30%. For silicon HJ, hydrogenated amorphous silicon films a few nanometers thick are good candidates for use as buffer layers since their bandgap is slightly wider than that of cSi[14]. They can be easily doped to make heterojunctions. For silicon HJ devices the following values are received in Ref. [7], V_{oc} =723 mV, J_{sc} =41.8 mA/cm^2 and FF=77.4%. Silicon heterojunction SCs, consisting of thin layers of amorphous silicon deposited on cSi wafers, provide an energy conversion efficiency of 21%[15]. In HJ, charge passes through this buffer layer slowly enough to produce a high voltage, but fast enough to avoid carrier recombination before collection. The buffer layer plays the role of a translucent membrane for the extraction of carriers[16]. In fact, both amorphous silicon and black silicon can act as buffer layers, and given the certain advantages of black silicon, it can also be used as buffer layers.

As is known, to convert solar radiation it is proposed to use tandem structures (for example, p-NiO (as HTM) – PVK – n-TiO_2 (as ETM) – p/bSi – p/cSi, here HTM, ETN, PVK and cSi means hole transfer material, electron transfer material, perovskite and crystalline silicon, correspondingly). Their benefits are well known[17-21]. The use of bSi in combination with cSi and perovskite layer has been shown to significantly improve the efficiency of solar cells[4, 18-28]. In above noted structure the created isotype heterojunction p-bSi with p-cSi will significantly contribute to the expansion of the absorption spectrum towards short waves. Such a displacement (expansion) can fill the region ("gap") between the absorption spectra of the upper layer of the PVK element and the lower layer of cSi. As a result, the efficiency of the element will increase. We will explore the possibility and efficiency of using the p-NiO – PVK – n-TiO_2 – bSi – cSi structure as a SC (Fig. 1).

In a recently published paper (see Ref. [17]), we investigated the optical properties and current voltage characteristics of the upper part of the proposed multilayer structure shown in Fig. 1, namely p-i-n structure made of PVK with intrinsic conductivity under irradiation. It is shown that both the short-circuit current and the open-circuit voltage take on rather large values. The potential possibility of using PVK in the design of tandem solar cells for converting solar energy is shown. Features of current flow in a perovskite/TiO_2 heterojunction are analyzed in Ref. [29].

In Fig. 1 schematic structure (a) and its energy diagram (b) of tandem SC under study are presented. The band gaps energies, affinity energies and Fermi energy for the corresponding regions of the tandem SC under study, as well as the energy of the vacuum level are shown in Fig. 2.

As it is known the band gap width of black Si is larger than that of crystalline Si. This is consistent with the formation of nanocrystalline Si. As noted in Ref. [25] conduction band minimum of p-bSi is 0.4 eV above that of p-type cSi results from the CPD (Continuing Professional Development) measurement. In the other hand since the bSi is directly grown on the very p-type Si, the distance between the Fermi energy level and the valence band maximum should basically be kept the same as the doping concentration is the same[10]. In further for band

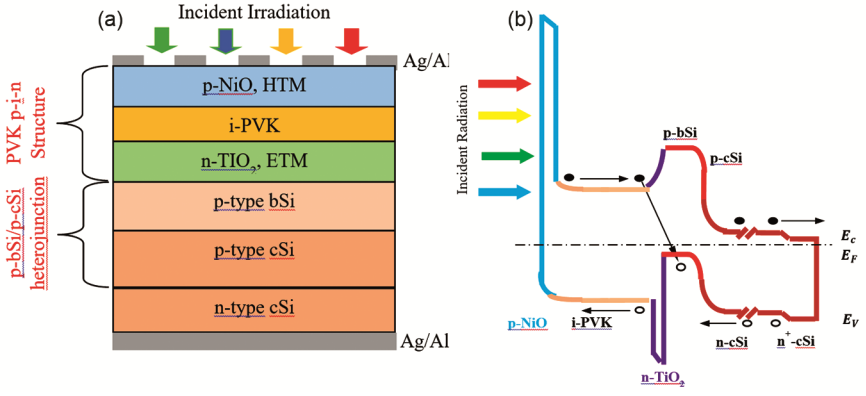

Fig. 1 — Schematic representation of the tandem solar cell (a), and energy diagram of a tandem solar cell (b) Here E_c. E_V and E_F are the energies of the bottom of the conduction band, the top of the valence band, and the Fermi energy, respectively

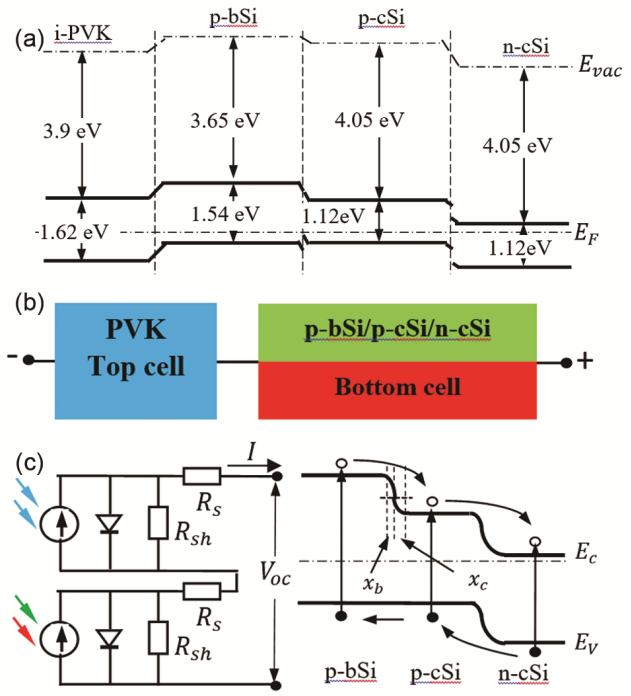

Fig. 2 — 2T PVK – bSi – cSi tandem SC energy diagram (a), its equivalent circuit (b) and p-bSi – p-cSi/n-cSi heterojunction (c)

gap energy of bSi we will used value1.54 eV[28]. The change in band gap energy of black silicon from crystalline silicon can also be justified using the similarities between black silicon and porous silicon. From the experimental data set, the electrical band-gap energy of porous Si is deduced to be (1.80 ± 0.01) eV, independent of sample temperature[30]. The energy gap in porous Si increased. The main factor for this is the quantum confinement effect.

The surface termination of the nanostructured Si also affects the band structure and hence the energy gap. This is explained for Si nanocrystals[31].

Figure 2 show 2T PVK – bSi - cSi tandem SC energy diagram (Fig. 2(a)), its equivalent circuit (Fig. 2(b)), and p-bSi/p-cSi heterojunction (Fig. 2(c)). Here I is the total current throw SC, R_s and R_{sh} are the serial and shunt resistances, x_b and x_c are thickness of depleted layers in p-bSi and p-cSi, correspondingly.

As can be seen from Figs. 1 & 2, the tandem solar cell under consideration can be formally represented as 2T (2 terminal) structure. Top part of equivalent scheme corresponds to PVK top cell, bottom part corresponds to silicon (p-bSi/p-cSi/n-cSi) bottom cell. To fully understand the processes of current flow in the complex structure of a SC noted above, in addition to studying the upper part (p-i-n structures, see Ref. [17]), it is also necessary to examine the lower part (p-p heterojunction).

In this paper, theoretical simulation of the current transfer process in the p-type black silicon/p-type crystalline silicon isotype heterojunction was carried out to optimize the optical and electrical parameters for using in solar energy conversion. We investigate the performance of the p-bSi/p-cSi part of a solar cell of the p-NiO – i-PVK – n-TiO_2 – p-bSi – p-cSi – n-cSi complex structure to improve light absorption and hence its photovoltaic performance.

2 Methodology of calculation of current-voltage characteristic and open circuit voltage for 2T tandem SC under condition of current matching

Current density J_{pin} for p-i-n PVK top cell of SC, presented in Fig. 1, is recently calculated by us[17]. It is following:

$$J_{pin}(\lambda) = J_s\left[exp\left(\frac{eV}{mkT}\right) - 1\right] - \frac{edP_{VK}(b+1)}{(b-1)}\left\{\Delta n\frac{\tau_n+\tau_p}{\tau_n\tau_p} - \frac{2\eta(\lambda)F_0}{d_{PVK}}[1exp(-\alpha_{PVK}x)]\right\}. \quad \ldots (1)$$

Here J_s is the saturation current

$$J_s = e\left(\frac{D_n n_p}{L_n} + \frac{D_p p_n}{L_p}\right) = kT\left(\frac{\mu_n n_p}{L_n} + \frac{\mu_p p_n}{L_p}\right), \quad \ldots (2)$$

m is the junction ideality factor, d_{PVK} is the thickness of PVK layer, $b = \mu_n/\mu_p$, $\mu_{n(p)}$, $\tau_{n(p)}$ and $D_{n(p)}$ are the mobility, lifetimes and diffusion constants of electrons (holes) in PVK, correspondingly, $\Delta n = \Delta p$ is the concentration of photocarriers and α_{PVK} is the PVK absorption coefficient, V is the voltage.

Since the bSi is directly grown on the very p-type cSi, the distance between the Fermi energy level and the valence band maximum should basically be kept the same as the doping concentration is the same[10]. In the Fig. 2(c) the p-bSi/p-cSi heterojunction formation is presented. Due to the equality of the maximum of the valence bands of p-bSi and p-cSi in this region, the internal built-in electric field separating photogenerated electrons and holes will be determined by the difference in bottom of the conduction bands bSi and cSi.

Let us assume that the dominant mechanism of current transfer in p-bSi/p-cSi isotype heterojunction is thermionic Anderson's emission model[32, 33]. Current-voltage characteristic of the isotype heterojunction under irradiation coming from bSi side is following[34]:

$$J_{p-p} = eN_{A,b(c)}\sqrt{\frac{D_{n,b}}{\tau_{n,b}}}\left[exp\left(\frac{eV_2}{kT}\right) - exp\left(-\frac{eV_1}{kT}\right)\right] - e\eta(\lambda)\big(1-R(\lambda)\big)[F_b e^{-\alpha_b x_b} + F_c e^{-\alpha_c x_c}] \quad \ldots (3)$$

Here $N_{A,b(c)}$ is the acceptor concentration in bSi is the same as in cSi, $D_{n,b}$ and $\tau_{n,b}$ are diffusion constant and lifetime of electrons in bSi, $R(\lambda)$ is the reflection coefficient of bSi, V_1 and V_2 parts of the applied voltage attributable to semiconductors p-bSi and p-cSi ($V_1 + V_2 = V$), F_b and F_c are the incident irradiation intensities in bSi and cSi ($F_c < F_b$), $\alpha_b(\lambda)$ and $\alpha_c(\lambda)$ are irradiation absorption coefficients in bSi and cSi, correspondingly,

$$x_b = \sqrt{\frac{2\varepsilon_0\varepsilon_b}{e^2 p_0}(\Phi_b - \Phi_c)}\,,\; x_c = \sqrt{\frac{2\varepsilon_0\varepsilon_c}{e^2 p_0}\left(\Phi_b - \Phi_c\right)} \ldots (4)$$

are the thickness of the depletion layers in bSi and in cSi by the minority carriers (see Fig. 2(c)), correspondingly, ε_0, ε_b and ε_c are vacuum constant, dielectric permittivity and Φ_b and Φ_c are work functions of bSi and cSi, correspondingly, p_0 is the majority carrier's concentration. Considering that the thickness of the bSi (usually about 4×10^{-5} cm) is much smaller than the thickness of the cSi (3×10^{-2} cm), it can be assumed that the generated photocarriers in both bSi and cSi parts will be partially separated by the internal built-in field of the isotype heterojunction and further partially by the p-n junction.

It is accepted that the matching of tandem batteries is studied from the point of view of the current matching condition[4]. It is clear that in this case the short circuit currents of the subelements must be equal. The current of a 2T tandem cell is limited to the cell that produces the lower current. The cell producing the higher current is limited to this lower current and operates at a voltage above its MPP (Maximum Power Point). As a result, the voltage of the tandem element increases slightly, but due to the low current, the efficiency value decreases (see later, data of the Table 1). It is also known that if a cell produces less current and has worse rectification, then a cell with a higher current can "push" part of its current through the limiting cell. In this case, the short current density J_{sc} of the tandem cell will increase to a value exceeding the J_{sc} of the limiting cell. Given the latter stated, assume that the lower current in the 2T cell is the current of the p-i-n bottom cell with current density J_{pin}. In this case total current density through SC according to current matching principle can be presented as the following:

$$J = J_{p-p} = J_{pin}.$$

The current mismatching ΔJ_{sc} quantify will by the difference between the current densities of the top and the bottom cells (see also Ref. [35]):

$$\Delta J_{sc} = J_{sc,p-p} - J_{sc,pin}.$$

Next we will calculate open circuit voltage V_{oc} as a sum of open circuit voltages of top and bottom cells (see, Fig. 2(c)):

$$V_{oc} = V_{oc,pin} + V_{oc,p-p}. \quad \ldots (5)$$

Expression of the $V_{oc,pin}$ is calculated from Eqn.(1) using condution $J_{pin}(\lambda) = 0$, which give us following:

$$V_{oc,pin} = \frac{mkT}{e} ln\left\{1 + \frac{ed_{PVK}(b+1)}{(b-1)J_s}\left\{\Delta n\frac{\tau_n+\tau_p}{\tau_n\tau_p} - \frac{2\eta(\lambda)F_0}{d_{PVK}}[1 - exp(-\alpha_{PVK}x)]\right\}\right\}. \quad \ldots (6)$$

The fill factor (FF) and the power conversion efficiency (PCE) will be calculated according to methodology developed in Ref. [17]:

$$\text{FF} = \frac{J_{mp}V_{mp}}{J_{sc}V_{oc}}; \quad \text{PCE} = \frac{J_{mp}V_{mp}}{P_i}. \quad \ldots (7)$$

Here J_{mp}, V_{mp} and P_i are maximum power current, maximum power voltage and the input power density, correspondingly, $V_{mp} \approx 0.9V_{oc}$, $J_{mp} = J$ at the $V \equiv V_{mp}$.

3 Numerical simulation

For numerical simulation of the open circuit voltage V_{oc}, short circuit current I_{sc} we need to collect and complete all electrical, optical and geometrical parameters of bSi and cSi[6, 10, 18-21, 28, 36]: $\rho = 3\,\Omega$cm, $\varepsilon_{cSi} = 11.7$, $\varepsilon_{bSi} \approx 8$, $\Phi_{cSi} = 4.9$ eV, $\Phi_{bSi} = 4.92$ eV, $\mu_p = 4.8 \times 10^2$ cm^2/Vs, $d_{bSi} = 4 \times 10^{-5}$ cm; $d_{cSi} = 3 \times 10^{-2}$ cm, $N_{A,bSi} = p_p = \frac{1}{e\mu_p\rho} = 4.3 \times 10^{15}$ cm^{-3}

Table 1 — Calculated values of J_{sc}, J_{mp}, V_{oc}, V_{mp}, FF and PCE for SC on the base of heterojunction p-bSi/p-cSi for several wavelengths.

λ, nm	300	400	500	600	700	800	900	1000
J_{sc}, mA/cm^2	4.4	13.2	23.6	28.7	31.0	20.0	15.8	14.0
J_{mp}, mA/cm^2	4.1	12.23	21.9	26.7	28,8	18.6	14.7	13.0
V_{oc}, mV	524	606	626	631	634	612	606	606
V_{mp}, mV	472	545	563	568	571	551	545	534
FF, %	84.5	85.31	85.9	85.9	86.4	86.5	85.4	85.0
PCE, %	1.89	6.59	12.3	15.1	16.4	10.3	7.9	6.8

(we use $N_{A,bSi} = 2 \times 10^{15}$ cm^{-3}), $P_i = 1$ kW/m^2=10^2 mW/cm^2. The energy flux of sunlight reaching the surface of the earth is 1.388×10^3 W/m^2. For bSi bandgap energy $E_g = 1.54$ eV and photon flux is equal to $F_b = 1.388 \times 10^3$ Wm^{-2}/1.54 eV = 5.6×10^{17}cm^{-2}s^{-1}. Considering that upon penetration of radiation it is partially weakened, in calculations we use $F_b = 2 \times 10^{17}$ cm^{-2}s^{-1} and $F_c = 1.6 \times 10^{17}$cm^{-2}s^{-1} According to (4) we find $x_b = 1.167 \times 10^{-5}$ cm; $x_c = 1.411 \times 10^{-5}$ cm.

For calculation we need also spectral dependencies of absorption coefficients of bSi and cSi. Using data from Fig. 4 in Ref. [37] for the spectrum region $0.7 < \lambda < 1.1$ μm we can approximate dependency $\alpha_{cSi}(\lambda)$. Considering that in heavily doped semiconductors with indirect transitions during optical transitions, the law of conservation of momentum can also be implemented due to the processes of electron-electron and electron-phonon scattering, the absorption coefficient can be represented in the form

$$\alpha_{cSi}(\lambda) \approx 6.3 \times 10^3 \times \left(\frac{1.234}{\lambda} - 1.12\right)^2 \quad \ldots (8)$$

Assuming that the behavior of $\alpha_{bSi}(\lambda)$ corresponds to the behavior of the absorption of cSi, for the spectral region $0.4 < \lambda < 0.8$ μm (see Refs. [18-20, 37]) we obtain the following approximate dependence for $\alpha_{bSi}(\lambda)$:

$$\alpha_{bSi}(\lambda) \approx 3.2 \times 10^4 \times \left(\frac{1.234}{\lambda} - 1.54\right)^2 \quad \ldots (9)$$

In (8) and (9) absorption coefficients $\alpha_{cSi}(\lambda)$ and $\alpha_{bSi}(\lambda)$ are given in cm^{-1}, and λ is given in μm.

4 Results and Conclusions

Results of the numerical calculation of current-voltage characteristics and spectral dependencies of the fill factor, short circuit current and open circuit voltage for the wavelength range 300-1000 nm of irradiation are presented in the Figs. 3-5. The curves were plotted using formulas (3), (6) and (7) using "Microsoft Excel spreadsheet software" according to the following method. To take into account the mechanisms of irradiation absorption in both bSi and cSi, in the wavelength range 700-1000 nm, is used expression (9) for the absorption coefficient cSi and in the wavelength range 300-700 nm, expressions for the absorption coefficient for bSi (8) are used.

In the Table 1 data for short circuit current density, open circuit voltage, maximum power current, maximum power voltage, FF and PCE for the

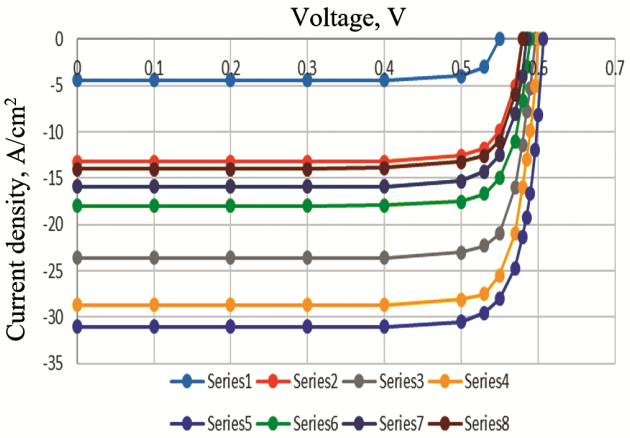

Fig. 3 — Current-voltage characteristic of p-bSi/p-cSi isotype heterojunction SC. Curves corresponds following wavelengths of irradiation: 300 nm (Series1), 400 nm (Series2), 500 nm (Series3), 600 nm (Series4), 700 nm (Series5), 800 nm (Series6), 900 nm (Series7), 1000 nm (Series8).

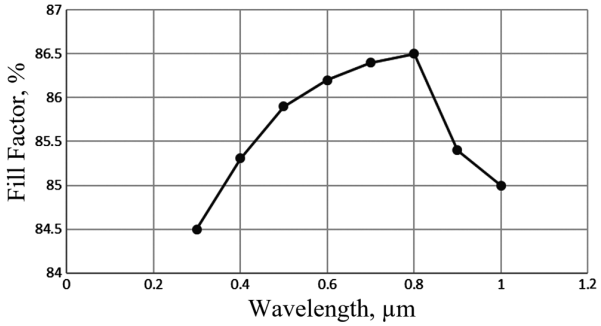

Fig. 4 — Spectral dependency of the fill factor

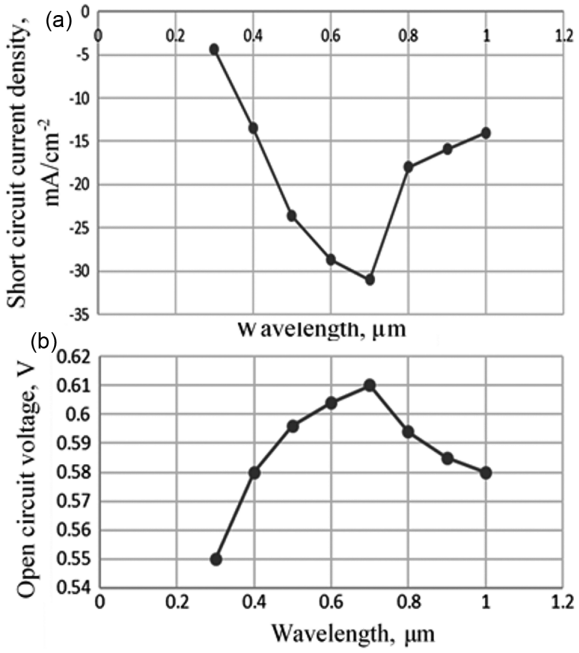

Fig. 5 — (a) Spectral dependency of short circuit current density (b) open circuit voltage

wavelength range 300-1000 nm are presented. Received data is in good agreement with the known reference results. Comparatively low values of short-circuit current at the low (300-400 nm) and high (900-1000 nm) wavelengths probably conditioned by the falling values of the absorption coefficients, both bSi and cSi (see Fig. 4 in Ref. [37]). The sharp changes in FF, J_{sc} and V_{oc} observed in Fig. 4, Fig. 5(a & b) in the wavelength range of 700-800 nm are most likely due to differences in the values of α_{cSi} and α_{bSi} in the transition region of wavelengths. In this region, with increasing wavelength, the absorption of bSi begins to decrease, and the absorption of cSi begins to increase, and due to the difference in the values of α_{cSi} and α_{bSi}, the evenness of the behavior of the graphs is disrupted. Recall that expression (8) for α_{cSi} is "valid" in the wavelength range of 700-1100 nm, and expression (9) for α_{bSi} is "valid" in the wavelength range of 300-800 nm."

Comparing the data obtained for PVK p-i-n structure from Ref. [17] and the data of Table 1, the following can be noted. For a 2T tandem fault shown in Fig. 2(b), according to the current matching in the wavelength range 700-800 nm, both the upper and lower parts (p-i-n structure and p-p heterojunction) short circuits demonstrate approximately the same values of the short circuit current. For the V_{oc} we must sum 634 mV (p-p heterojunction) with 1030 mV (p-i-n structure[17]) for a wavelength of 700 nm and, respectively, 612 mV and 990 mV for a wavelength of 800 nm. As a result, for the open circuit voltage in the wavelength range 700-800 nm we obtain 1.664-1.602 V. This means $V_{oc} = 1.602 \div 1.664$ V. For the PCE we have correspondingly 41.5 % ($\lambda = 700$ nm) and PCE=27.9 % ($\lambda = 800$ nm). Such values of the power conversion efficiency suggest successful use of the SC design proposed in Fig. 1, for efficient solar energy conversion.

Obtained values for the open circuit voltage are in good agreement with literature data (for example Ref. [37]). For similar tandem structures, the following values for photoelectric parameters were obtained[4]: open circuit voltage 1.779 V, short circuit current density 20.19 mA/cm^2, fill factor 82.22 %, and efficiency 28.50 %, respectively. According Ref. [38] for Oh's p-type solar cells $J_{sc} \propto 26.62$ mA/cm^2 and $V_{oc} \propto 617$ mV (polished silicon), and $J_{sc} \propto 38.26$ mA/cm^2 and $V_{oc} \propto 624$ mV (pyramid textured Si with 110 nm SiN_x coating).

Figure 4 shows spectral dependency of the FF. Good values (>85 %) are obtained in the wavelength range 400-1000 nm.

Spectral dependencies of the short circuit current and open circuit voltage are shown in Figs. 5(a & b).

Thus it is demonstrated the possibility of using thin layers of black silicon to convert solar energy. It is shown that in combination with the crystalline silicon, black silicon can broaden the absorption spectrum of irradiation, thereby increasing the power conversion efficiency of the tandem solar cells.

Funding: The investigation is carried out with the financial support of the Science Committee of the Republic of Armenia within the framework of Scientific Project No. 21AG-2B011.

Data Availability: The data that support the findings of this study are available within the article.

Competing Interests: The authors declare no competing financial interest.

References

1 Savin H, Repo P, Gastrow G, Ortega P, Calle E, Garín M & Alcubilla R, *Nature Nanotechnolog,* 10 (2015) 624.
2 Bett A J, Eisenlohr J., Höhn O, Repo P, Savin H, Bläsi B & Goldschmidt J C, *Opt Express*, 24 (2016) A434.
3 Onyshchenko V F, Karachevtseva L A, Lytvynenko O O, Plakhotnyuk m M & Stronska O J, *Semicond Physics Quant Electron Optoelectron,* 20 (2017) 325.
4 Ayvazyan G E, Black Silicon Formation, Properties, and Application, Springer, 2024.
5 Bett A J, Eisenlohr J, Höhn O, Repo P, Savin H, Bläsi & Goldschmidt J C, *Opt Express*, 24 (2016) A434.
6 Zhao Z, Zhang Z, Jin J, *et al*., *APL Mater,* 11 (2023) 021107.
7 Zhang Y, Loh J Y Y & Kherani N P, *Adv Sci*, 8 (2022) 2203234.
8 Chai J Y-H, Wong B T, Juodkazis S, *Mater Today Energy*, 18 (2020) 100539.
9 Tsang T, Bolotnikov A, Haarahiltunen A & Heinonen J, *Opt Express*, 28 (2020) 13299.
10 Garin M, Heinonen J, Werner L, Pasanen T P, Vähänissi V, Haarahiltunen A, Juntunen M A & Savin H, *Phys Rev Lett*, 12 (2020) 117702.
11 Hamakawa Y, Fujimoto K, Okuda K, Kashima Y, Nonomura S & Okamoto H, *Appl Phys Lett*, 43 (1983) 644.
12 Spear W E & LeComber P G, *Solid State Commun*, 17 (1975) 1193.
13 Lin H, Yang M, Ru X, *et al*., *Nat Energy* 8, (2023) 789.
14 De Wolf S, Descoeudres A, Holman Za C & Ballif C, *Green*, 2 (2012) 7.
15 Würfel P, Physics of Solar Cells, From Principles to New Concepts, Wiley-WCH, Weinheim, 2005.
16 Ji S, Syn H, Choi J, Lee H M and Kim D, Tech Digest 21st Int *Photovolt Sci Eng Conf*, Fukuoka, Japan, (2011) 3A-1O-06.
17 Gasparyan F, *Indian J Pure Appl Phys*, 62 (2024) 51.
18 Gasparyan F, *Adv Mater Sci Technol*, 5 (2023) 0517626.

19 Ayvazyan G, Gasparyan F & Gasparian V, *Opt Mater*, 140 (2023) 113879.
20 Ayvazyan G, Vaseashta A, Gasparyan F, Khudaverdyan S, *J Mater Sci: Mater Electron,* 33 (2022) 17001.
21 Gasparyan F V & Ayvazyan G Y, *J Contemp Phys*, 57 (2022) 160.
22 Akhil S, Akash S, Pasha A, Kulkarni B, Jalalah M, Alsaiari M, Harraz F A & Balakrishna R G, *Mater Design*, 211 (2021) 110138.
23 Zhao Y, Ma F, Qu Z, Yu S, Shen T, Deng H X, Chu X, Peng X, Yuan Y & Zhang X*, Science,* 377 (2022) 531.
24 *Zhou Z-Q, Hu F, Zhou W-J, Chen H-Y, Ma L, Zhang C & Lu M, Nano Express, 12 (2017) 623.*
25 Grundmann M, The Physics of Semiconductors, An Introduction Including Nanophysics and Applications, 2010.
26 Hwail H M & Abdullah M M, *EUREKA: Phys Eng*, 4 (2021) 134.
27 Zhou Z Q, Hu F, Zhou W J, *et al*., *Nanoscale Res Lett*, 12 (2017) 1.
28 Frederiksen J T, Melcher P G & Veje E, *J Porous Mater*, 7 (2000) 271.
29 Gevorkian Z, Gasparian V & Lozovik Y, *Appl Phys Lett*, 108 (2016) 051109.
30 Praveenkumar S, Lingaraja D, Mahiz M P & Dinesh R G, *Optik*, 178 (2019) 216.
31 Sze S M & Ng K K, Physics of Semiconductor Devices, 3rd Edn, John Wiley & Sons, (2007).
32 Anderson R L, *Solid State Electron*, 5 (1962) 841.
33 Park M S, Irradiation effect in triple junction solar cells for spatial applications, *Theses*, 2018.
34 Sharma B L & Purohit R K, Semiconductor heterojunctions, Pergamon Press, 1974.
35 Ašmontas S & Mujahid M, *Nanomaterials*, *13* (2023) 1886.
36 Afrasiab, Khan A D, Subhan F E, Khan A D, Khan S D, Ahma M S, Rehan M S & Noman M, *Optik,* 208 (2020) 164573.
37 Liu X, Coxon P R, Peters M, Hoex B, Cole J M & Fray D J, *Energy Environ Sci*, 10 (2014) 3223.
38 Oh J, Yuan H C & Branz H M, *Nat Nanotechnol*, **7** (2012) 743.